Full length article

Effects of hip joint centre mislocation on gait kinematics of children with cerebral palsy calculated using patient-specific direct and inverse kinematic models

Hans Kainz[a,b,c,d], Christopher P. Carty[a,b,c], Sheanna Maine[c], Henry P.J. Walsh[c], David G. Lloyd[a,b], Luca Modenese[a,b,e,f,*]

[a] School of Allied Health Sciences, Menzies Health Institute Queensland, Griffith University, Gold Coast, Australia
[b] Centre for Musculoskeletal Research, Menzies Health Institute Queensland, Griffith University, Gold Coast, Australia
[c] Queensland Children's Motion Analysis Service, Queensland Paediatric Rehabilitation Service, Children's Health Queensland Hospital and Health Services, Brisbane, Australia
[d] Department of Kinesiology, KU Leuven, Leuven, Belgium
[e] Department of Mechanical Engineering, The University of Sheffield, United Kingdom
[f] INSIGNEO Institute for In Silico Medicine, The University of Sheffield, United Kingdom

ARTICLE INFO

ABSTRACT

Joint kinematics can be calculated by Direct Kinematics (DK), which is used in most clinical gait laboratories, or Inverse Kinematics (IK), which is mainly used for musculoskeletal research. In both approaches, joint centre locations are required to compute joint angles. The hip joint centre (HJC) in DK models can be estimated using predictive or functional methods, while in IK models can be obtained by scaling generic models. The aim of the current study was to systematically investigate the impact of HJC location errors on lower limb joint kinematics of a clinical population using DK and IK approaches. Subject-specific kinematic models of eight children with cerebral palsy were built from magnetic resonance images and used as reference models. HJC was then perturbed in 6 mm steps within a 60 mm cubic grid, and kinematic waveforms were calculated for the reference and perturbed models. HJC perturbations affected only hip and knee joint kinematics in a DK framework, but all joint angles were affected when using IK. In the DK model, joint constraints increased the sensitivity of joint range-of-motion to HJC location errors. Mean joint angle offsets larger than 5° were observed for both approaches (DK and IK), which were larger than previously reported for healthy adults. In the absence of medical images to identify the HJC, predictive or functional methods with small errors in anterior-posterior and medial-lateral directions and scaling procedures minimizing HJC location errors in the anterior-posterior direction should be chosen to minimize the impact on joint kinematics.

1. Introduction

In children with cerebral palsy (CP), three-dimensional gait analysis is used for treatment planning and evaluating the outcome of an intervention [1]. Most clinical gait laboratories use variants of the conventional gait model [2,3], included in most commercially available motion capture systems. Joint kinematics are calculated by the conventional gait model as Cardan angles describing the relative pose of adjacent anatomical segment reference systems, which are defined from the experimental markers' positions and a minimum set of anatomical measurements (Direct Kinematics, DK) [4,5]. Conversely, musculoskeletal software such as AnyBody [6] and OpenSim [7] use an Inverse

Kinematics (IK) approach to compute joint angles from marker trajectories. In the IK framework, also known as "global optimization" or "multi-body optimization", joint angles are calculated by adjusting the pose of a scaled musculoskeletal model to best match the model markers' position with the experimental surface markers at each frame of their trajectory [8,9]. Musculoskeletal software may provide valuable additional information on the causes of gait abnormalities and therefore improve clinical-decision making because it allows additional analyses such as musculotendon length estimation [10,11], joint contact force calculations [12,13] and induced acceleration analysis [14].

Kinematic models usually differ between DK and IK approaches. Most currently available lower body IK models use constrained joints,

i.e. 3 degrees of freedom (DoF) joint (ball-and-socket joint) at the hip and a 1 DoF joint at the knee and talocrural joint [15–17]. Alternatively, DK approaches can have constrained and unconstrained, i.e. 6 DoF, joint models [2,18,19]. Both DK and IK approaches, however, require joint centre locations for kinematic and kinetic analyses. The hip joint centre (HJC) is difficult to estimate because it is not a palpable bony landmark, so in conventional gait models predictive or functional methods are used to estimate its location in the pelvis reference system [20], whereas in musculoskeletal models its location is defined by scaling the pelvis segment [7].

When using a DK approach, HJC location errors can lead to an offset (change in mean angle) and, depending on the direction of the mislocation, to a distortion (change in ranges of motion, ROM) of the estimated lower limb joint kinematics [19,21]. To the authors' knowledge, no studies have evaluated the impact of HJC location errors on joint kinematics using an IK approach. However, using unconstrained DK models for healthy adults HJC location errors had negligible effect on mean and ROM's of estimated hip and knee angles, i.e. < 1.5°, [21], while in constrained DK models HJC errors had large effects on hip joint ROM; up to 6.7° [19], which could be indicative of HJC location errors on IK estimated lower limb joint kinematics. Furthermore, the DK results were obtained for healthy adults, and the results may be different for paediatric patient populations, for which there are no studies yet.

Therefore, this study aimed to investigate the propagation of HJC location errors to mean and ROM in the lower limb joint kinematics of children with CP using DK and IK models with different joint constraints. It was hypothesised that HJC location errors affect mean and ROM of all joint angles in IK models, whereas only hip and knee kinematics will be affected in the DK models.

2. Methods

2.1. Participants

Three children with hemiplegic and five children with diplegic CP (four males, four females; age: 10 ± 3years, height: 1.30 ± 0.15 m, mass: 27 ± 6 kg, body mass index: 16 ± 1 kg/m^2, GMFCS level 1–3) were recruited and presented for motion capture and magnetic resonance imaging (MRI) data collection sessions. None of the participants required an assistive device for walking. Ethics approval was obtained from the Queensland Children's Health Services Human Research Ethics Committee, and parents gave their informed and written consent for their children to participate in the study.

2.2. Motion capture and MRI imaging

Motion capture data was collected at the Queensland Children's Motion Analysis Service (Brisbane, Australia). A physiotherapist, experienced in clinical gait analysis, placed retro-reflective MRI-visible surface markers (Table 1) on each participant. An 8-camera, 3-dimensional motion capture system (Vicon Motion Systems, Oxford, UK) was used to collect one static calibration and at least six walking trials for each participant. To identify initial contact and foot-off gait events, ground reaction forces were simultaneously acquired using three force platforms (AMTI OR6-7-1000, Watertown, MA, USA). Vicon Nexus 1.8.5 (Vicon Motion Systems, Oxford, UK) was used to label and filter marker trajectories using a 4th order forward-reverse-pass zero-lag Butterworth low pass filter with cut-off frequency of 6 Hz. At the end of the motion data collection a waterproof pen was used to mark the position of the surface markers on the anatomical landmarks. In the same week of the gait analysis session, full lower-body MRI scans were collected from each participant in a supine position at the Royal Children's Hospital (Brisbane, Australia) or the Lady Cilento Children's Hospital (Brisbane, Australia). Prior to the MRI scans the same MRI-visible surface markers were placed on the marked positions on the pelvis, knee, ankle and foot of each participant. Images were collected with 1.5T magnetic resonance scanners (MAGNETOM Avanto, Siemens, Berlin/Munic, Germany) using a modified 3D Proton Density SPACE sequence (slice thickness 1.1 mm, slice increments 1.1 mm, voxel size 0.83 × 0.83 × 1.0 mm).

2.3. Kinematic models

Following the session in the gait lab and MRI data collection, lower limb kinematic waveforms were computed for both investigated methodologies using patient-specific models created from the MRIs.

2.3.1. IK models

The patient specific "reference models" were created by processing the collected MRI and motion capture data via four steps as reported in detail in our previous study [22]:

1. The skin, bones and MRI-visible surface markers of the right lower limb for each participant were segmented using Mimics (Materialise, Belgium).
2. The bone geometries were imported into 3-matics (Materialise, Belgium) and subject-specific joint parameters were calculated by fitting spheres to joint contact surfaces.
3. Bone geometries, marker centroids, and the joint centres and axes, were imported into NMSBuilder [23] from which subject-specific unilateral OpenSim models were created for all participants. These models included four segments (pelvis, thigh, shank, and foot) connected by three joints, with centres and axes described in [22]. Virtual markers, placed in the same position as the MRI visible markers, were also included in the model. Anatomical segment reference systems (ASRS) consistent with the recommendation of the International Society of Biomechanics [24] were defined (supplementary Table S1). Two IK models were created for each participant, the 3-1-1-DoF-IK and 3-3-3-DoF-IK model. In the 3-1-1-DoF-IK model, the hip joint had 3 DoF (flexion-extension, abd-adduction, and internal-external rotation), the knee 1 flexion-extension DoF, and ankle 1 planter-dorsiflexion DoF, while the pelvis had a 6 DoF free joint with ground. In the 3-3-3-DoF-IK model the hip, knee and ankle joints had 3 rotational DoF.
4. After creating the IK models, the marker placement tool available in OpenSim was used for registering the cluster markers (not available during the MRI scans) onto the model segments using the markers visible in the MRI as a reference.

Joint angles were calculated through the weighted least squares optimization available in OpenSim [7] assigning an equal weight to all tracking markers (Table 1).

2.3.2. DK models

DK models were generated from the finalised IK models. From the static pose data of the participants their model ASRSs were defined and stored into technical segment frames (TSF) defined by surface markers (Fig. 1). Subsequently, their pose matrix with respect to the proximal segment could be reconstructed in each frame and decomposed into Cardan angles (flexion-extension, abd-adduction, and internal-external rotation sequence). Two DK models were created for each subject. The 6-DoF-DK model, similar to [25], had no joint constraints between segments, whereas the 3-DoF-DK model only allowed joint rotations, similar to the conventional gait model [2,3]. Calculations were performed using a custom Matlab script (R2013a, The Math Works, Natick, USA).

2.4. Hip joint centre perturbation

For each trial, joint kinematics were first calculated using the reference models, i.e. with the HJC location defined from the MRIs, and then using modified models with altered HJC. The HJC coordinates

Table 1
Markers placed on the participants during the MRI, motion capture (MOCAP) session and used for kinematics analysis performed with the DK and IK models. The first three participants did not have the RD5M and LD5M markers. The RIC/LIC markers were used, in combination with the LASI and RASI markers, to adjust the position of the LPSI and RPSI markers in the MRI models in the case of a discrepancy in marker locations between the MRI images (collected in a supine position) and the static standing calibration trial.

Segment	Marker name	Anatomical description	Markers usage		
			MRI	MOCAP	Kinematic analysis
Pelvis	RASI/LASI	Right/left anterior superior iliac spine	Yes	Yes	Yes
	RPSI/LPSI	Right/left posterior superior iliac spine	Yes	Yes	Yes
	RIC/LIC	Right/left iliac crest	Yes	Yes	–
Thigh	RTH1/LTH1	Right/left thigh cluster marker 1	–	Yes	Yes
	RTH2/LTH2	Right/left thigh cluster marker 2	–	Yes	Yes
	RTH3/LTH3	Right/left thigh cluster marker 3	–	Yes	Yes
	RKNE/LKNE	Right/left lateral femoral epicondyle	Yes	Yes	–
	RMKNE/LMKNE	Right/left medial femoral epicondyle	Yes	Yes	–
Shank	RTB1/LTB1	Right/left shank cluster marker 1	–	Yes	Yes
	RTB2/LTB2	Right/left shank cluster marker 2	–	Yes	Yes
	RTB3/LTB3	Right/left shank cluster marker 3	–	Yes	Yes
	RANK/LANK	Right/left lateral malleolus	Yes	Yes	–
	RMMA/LMMA	Right/left medial malleolus	Yes	Yes	–
Foot	RTOE/LTOE	Top of the second metatarsal head	Yes	Yes	Yes
	RD5M/LD5M	Lateral aspect of the 5th metatarsal head	Yes	Yes	Yes
	RHEE/LHEE	Posterior aspect of the heel at the same height as the RTOE/LTOE marker	Yes	Yes	Yes

were perturbed using a cubical grid centred in the nominal HJC whose axes were aligned to the anterior-posterior (x-axis), superior-inferior (y-axis) and medial-lateral (z-axis) anatomical axes of the pelvis (supplementary Fig. S1). The cubic grid included all possible combinations of Δx, Δy and Δz errors, in the range of ± 30 mm [21,26] with 6 mm steps. A total of 1330 perturbed models for each DK and IK model were generated.

2.5. Data analysis

Similar to Stagni et al. [21], the offset, i.e. propagated error in the mean joint angles $\Delta\bar{q}$, was calculated by subtracting the mean value of a gait cycle of the reference model's kinematic waveforms from the mean value of the perturbed waveform. The change in joint ROM, i.e. propagated error of the peak-to-peak Δq_{pp}, was similarly calculated by subtracting the peak-to-peak of the reference model's waveform from the peak-to-peak of the perturbed waveform. Both values, $\Delta\bar{q}$ and Δq_{pp}, were correlated with the HJC perturbations (Δx, Δy, Δz). Results were

presented non-normalised (Δpeak = 1) and normalised to the absolute value of the maximum perturbation (Δpeak = 30 mm).

$$\Delta\bar{q} = m_x\left(\frac{\Delta x}{\Delta peak}\right) + m_y\left(\frac{\Delta y}{\Delta peak}\right) + m_z\left(\frac{\Delta z}{\Delta peak}\right)$$

$$\Delta q_{pp} = p_x\left(\frac{\Delta x}{\Delta peak}\right) + p_y\left(\frac{\Delta y}{\Delta peak}\right) + p_z\left(\frac{\Delta z}{\Delta peak}\right)$$

In these equations m_x, m_y, m_z, p_x, p_y and p_z are the regression coefficients from the multiple regression analyses, which represent the sensitivities of mean and ROM joint angles to HJC location errors. The offset, $\Delta\bar{q}$, and change in ROM, Δq_{pp}, of joint angles were calculated for every trial and the average values were used in the described regression analyses. Due to the large variability in CP gait kinematics (supplementary Fig. S2) regression coefficients were first calculated for each participant and then averaged over all participants to account for inter-subject variability. Differences in the regression coefficients between the 3-DoF-DK and 3-3-3-DoF-IK models were used to evaluate the impact of the computational method (DK vs. IK) on the HJC sensitivity. Differences in the regression coefficients between the 3-1-1-DoF-IK and
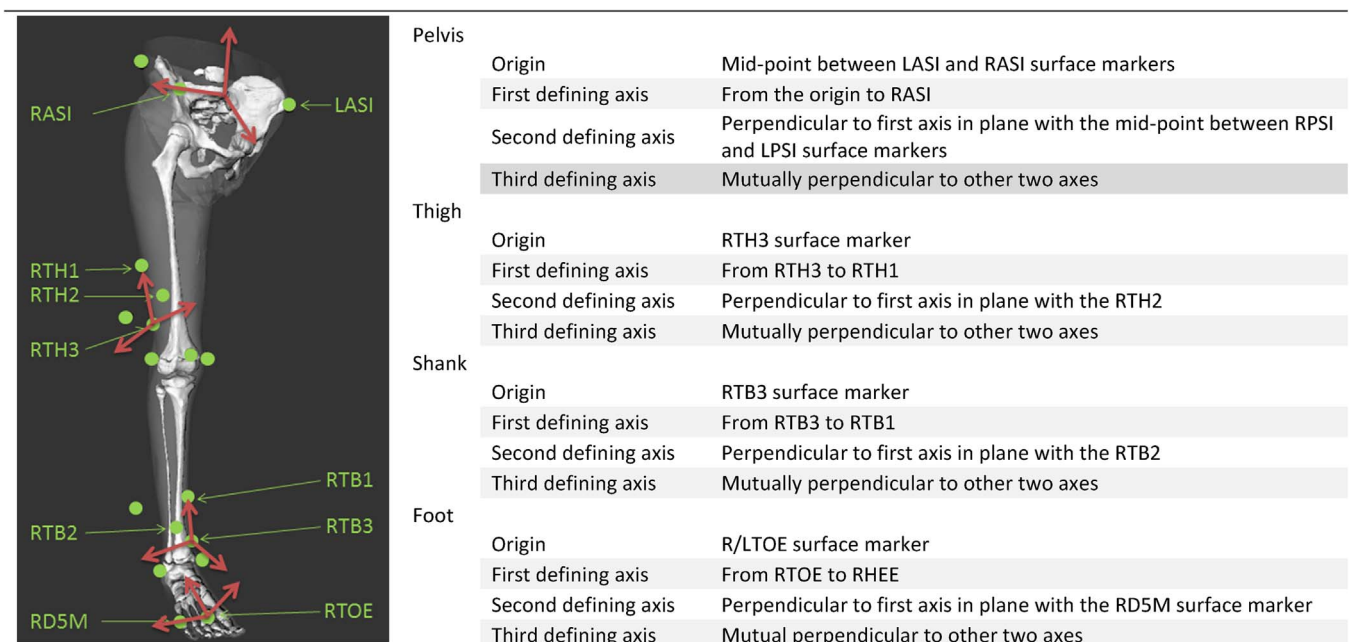

Pelvis		
	Origin	Mid-point between LASI and RASI surface markers
	First defining axis	From the origin to RASI
	Second defining axis	Perpendicular to first axis in plane with the mid-point between RPSI and LPSI surface markers
	Third defining axis	Mutually perpendicular to other two axes
Thigh		
	Origin	RTH3 surface marker
	First defining axis	From RTH3 to RTH1
	Second defining axis	Perpendicular to first axis in plane with the RTH2
	Third defining axis	Mutually perpendicular to other two axes
Shank		
	Origin	RTB3 surface marker
	First defining axis	From RTB3 to RTB1
	Second defining axis	Perpendicular to first axis in plane with the RTB2
	Third defining axis	Mutually perpendicular to other two axes
Foot		
	Origin	R/LTOE surface marker
	First defining axis	From RTOE to RHEE
	Second defining axis	Perpendicular to first axis in plane with the RD5M surface marker
	Third defining axis	Mutual perpendicular to other two axes

Fig. 1. Definitions of the technical segment frames (TSF). Definition of the anatomical segment frames can be found in the electronic Appendix Table S1.
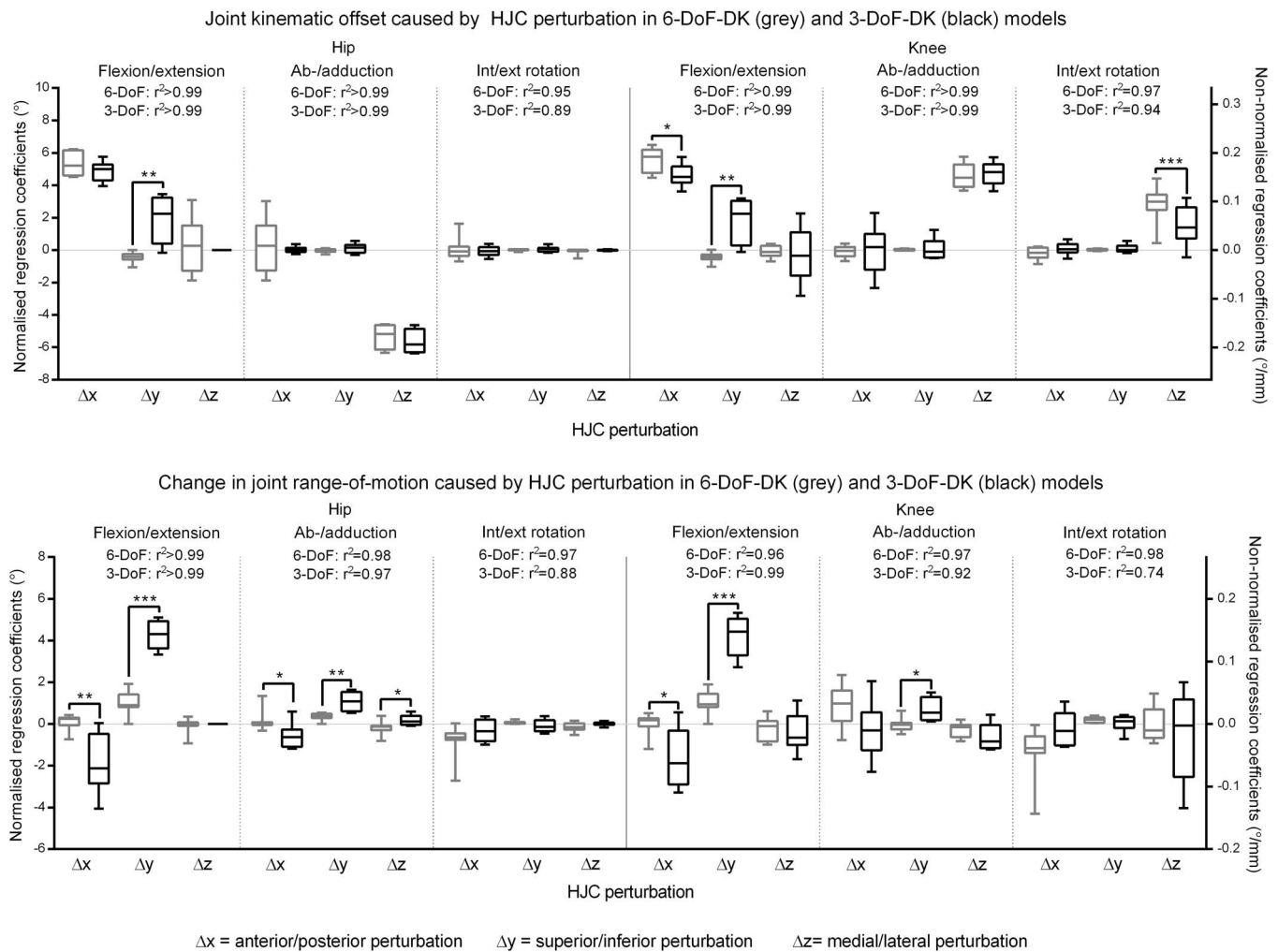
Joint kinematic offset caused by HJC perturbation in 6-DoF-DK (grey) and 3-DoF-DK (black) models

Change in joint range-of-motion caused by HJC perturbation in 6-DoF-DK (grey) and 3-DoF-DK (black) models

Δx = anterior/posterior perturbation   Δy = superior/inferior perturbation   Δz= medial/lateral perturbation

Fig. 2. Boxplots of the normalised (left Y-axis) and non-normalised (right Y-axis) regression coefficients obtained for the 6-DoF-DK (grey boxes) and 3-DoF-DK (black boxes) models. For each hip joint centre perturbation direction (Δx, Δy, Δz), the whisker runs from the minimum to the maximum regression coefficient for each joint angle across all participants. Mean coefficient of multiple determinations (r^2) are reported too. *,**,*** indicate significant differences (*$p < 0.05$, **$p < 0.01$, ***$p < 0.001$) between the regression coefficients obtained for the 3-DoF-DK and 6-DoF-DK models.

3-3-3-DoF-IK models, and between the 3-DoF-DK and 6-DoF-DK were used to analyse the impact of joint constraints on HJC sensitivity in IK and DK models, respectively. A repeated measures general linear model was used for each comparison and joint angle. In the case of significant interactions, post-hoc comparisons were performed using Bonferroni corrections. The significance level was $p < 0.05$ and IBM SPSS Statistics 21 (IBM Corporation, Ney York, USA) was used for all statistical analyses.

3. Results

HJC perturbations affected the DK and IK models in different ways (Fig. 2-4). For the DK models, HJC perturbations changed hip and knee kinematic waveforms but, as expected, did not alter pelvis or ankle kinematics. In DK models (6-DoF-DK and 3-DoF-DK), anterior-posterior HJC perturbations mainly affected mean hip and knee flexion-extension angles (ranging from 4 to 6.4 ° of variation for both models), whereas errors in the medial-lateral direction primarily influenced mean hip and knee ab-adduction angles (median variations larger than 5° for both joints) (Fig. 2). Changes in hip and knee flexion/extension joint ROMs were significantly larger ($p < 0.05$) in the 3-DoF-DK than in the 6-DoF-DK model, with variations exceeding 5° in the former model while never exceeding 2° in the latter. Superior/inferior and anterior/posterior HJC perturbations were causing the largest ROM variations.

For the IK models, HJC perturbations had an impact on all analysed joint angles with hip and knee angles being most sensitive to errors in the anterior-posterior direction and ankle angles being the least affected. Angle variations were up to 8.3° for the hip angles and up to 5.9° for knee flexion/extension. Over all joint angles, the changes in joint ROM and mean joint angles caused by HJC location errors were slightly smaller in the 3-1-1-DoF-IK than in the 3-3-3-DoF-IK models (Fig. 3). However, the differences at the hip joint were statistically significant only for flexion/extension, ab-/adduction and internal/external rotation angle variations caused by superior/inferior, anterior/posterior and medial/lateral perturbation respectively. Significant differences due to medial/lateral perturbation were also found for pelvis obliquity and knee flexion/extension angles.

The comparison between the 3-DoF-DK and 3-3-3-DoF-IK models identified significantly different sensitivities of mean joint angles to HJC perturbations for hip and knee joints (Fig. 4). In particular, HJC location errors in the medial/lateral direction caused significant differences in the hip and knee ab/adduction and knee internal/external rotation angles, while anterior-posterior and superior/inferior perturbations led to changes in the hip and knee flexion/extension. Finally, HJC perturbations in anterior-posterior and superior-inferior directions were responsible for significant differences between the ROM of hip flexion-extension and ab-adduction angles and all three rotations of the knee joint (Fig. 4).
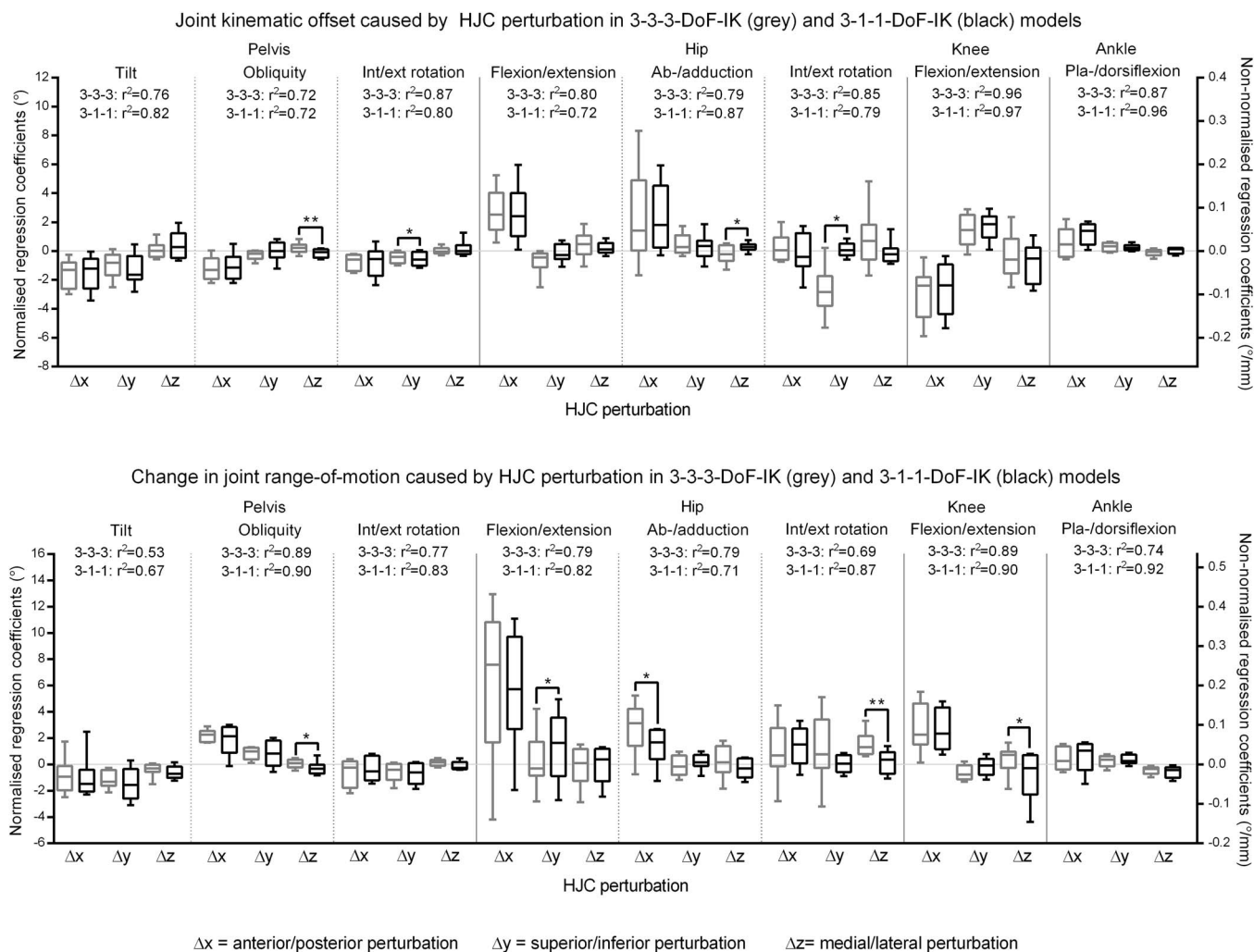
Fig. 3. Boxplots of the normalised (left Y-axis) and non-normalised (right Y-axis) regression coefficients obtained for the 3-3-3-DoF-IK (grey boxes) and 3-1-1-DoF-IK (black boxes) models. For each hip joint centre perturbation direction (Δx, Δy, Δz), the whisker runs from the minimum to the maximum regression coefficient for each joint angle across all participants. Mean coefficient of multiple determinations (r^2) are reported too. Regression coefficients for knee ab-/adduction and internal/external rotation for the 3-3-3-DoF-IK model are shown in Fig. 2. *,**,*** indicate significant differences (*$p < 0.05$, **$p < 0.01$, ***$p < 0.001$) between the regression coefficients obtained for the 3-3-3-DoF-IK and 3-1-1-DoF-IK models.

4. Discussion

This is the first study to evaluate the impact of HJC location errors on lower limb joint kinematics in children with CP when using DK and IK approaches. Using DK anterior-posterior and medial/lateral HJC location errors had the largest impact on joint kinematics leading to large and consistent offset of hip and knee flexion-extension and ab-adduction angles. Contrastingly, using the IK approach HJC location errors impacted all joint angles, but the propagated errors were generally more variable and dispersed across all joints.

Due to their computational dissimilarities the DK and IK approaches produced large differences in their mean offset and ROM joint angles sensitivities. DK calculations only involve adjacent ASRS, so HJC perturbations only affected the femur ASRS thereby altering hip and knee joint kinematics alone, while IK's global optimization affected all joint angles, confirming our hypothesis. Researchers and clinicians using IK modelling on similar populations should be aware that errors in locating the HJC will impact the kinematics of the entire lower limb kinematic chain, especially when the HJC location is not identified from medical images. Moreover, it is worth noting that the effect of HJC errors can combine with other methodological issues, making kinematic results challenging to interpret; in DK-models, for instance, medial/lateral perturbations cause changes in knee axial rotation that are not

matched by a corresponding hip joint axial rotation, due to the effect of order of rotation in pose decomposition.

We found that HJC location errors in DK models mainly affected hip flexion-extension and ab-adduction rotations with small influences on hip internal-external rotations. Furthermore, hip ROM errors in our 6-DoF-DK model (maximal error of 2.7°) were smaller than in our 3-DoF-DK model (maximal error of 5.1°). This is similar to Cereatti et al. [19] who found ROM errors up to 0.8° and 6.7° for an unconstrained (6-DoF) and constrained (3-DoF) DK model, respectively. The present study's IK models had ROM errors, i.e. waveform distortions, up to 12.9°, which were substantially larger than the maximum ROM errors in the DK models of 5.3°. Our IK and 3-DoF-DK models included joint constraints, similar to the constrained DK model in [19], and led to a shift and distortion of kinematic waveforms, whereas HJC perturbations in our unconstrained 6-DoF-DK model only offset the waveforms without distortion.

In contrast to our results, Stagni et al. [21] found that HJC location errors had negligible impact on mean hip and knee angles using DK methods. However, their study collected data from healthy adult participants, and in contrast, our children with CP had different hip and knee joint ROM (see kinematic waveforms in supplementary Fig. S3 and S4), and shorter femur lengths, which led to larger impact of HJC errors on joint kinematics. Furthermore, the ASRS in [21] were derived from
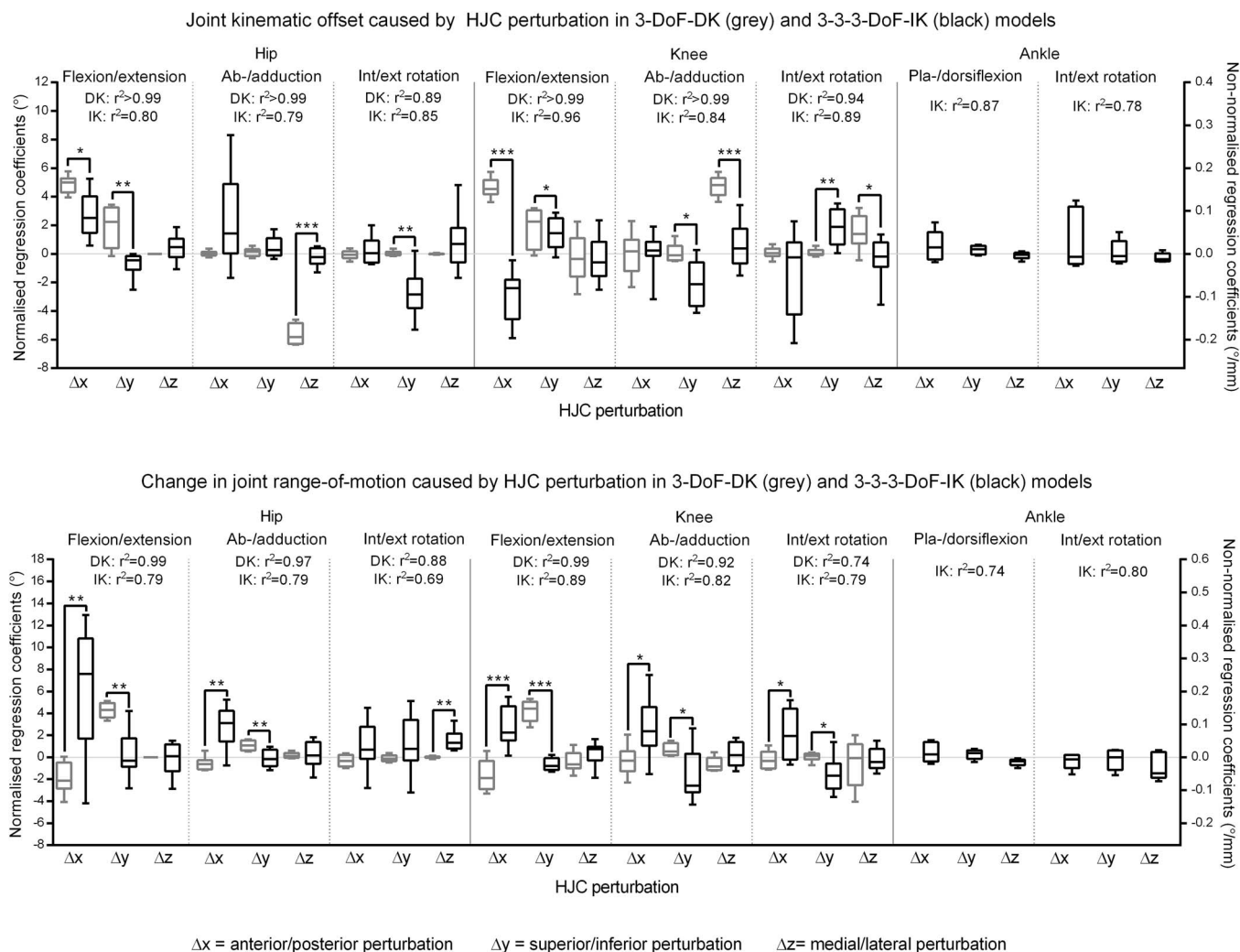
Fig. 4. Boxplots of the normalised (left Y-axis) and non-normalised (right Y-axis) regression coefficients obtained for the 3-DoF-DK (grey boxes) and 3-3-3-DoF-IK (black boxes) models. For each hip joint centre perturbation direction (Δx, Δy, Δz), the whisker runs from the minimum to the maximum regression coefficient for each joint angle across all participants. Mean coefficient of multiple determinations (r^2) are reported too. Regression coefficients for pelvic rotation for the 3-3-3-DoF-IK model are shown in Fig. 3. DK results for ankle joint kinematics are not reported because they are not affected by the HJC perturbation. *,**,*** indicate significant differences (*p < 0.05, **p < 0.01, ***p < 0.001) between the regression coefficients obtained for the 3-3-3-DoF-IK and 3-DoF-DK models.

the location of surface markers from a static standing trial whereas in our study the ASRS were created from MRIs in a supine position, which could cause different offsets between the ASRS and TSF. Comparing the angular offset between ASRS and TSF from the MRI models with the angular offset from models created using only the marker locations from a static trial showed a mean difference of 3.2°, which is insufficient to account for differences between our results and those presented in [21].

This study presents potential limitations that must be considered when interpreting our findings. MRIs were collected in a supine position, which moved the posterior superior iliac spine markers more superior in three participants due to a body pose adjustment after the participant laid down. However, having the additional iliac crest markers together with the anterior superior iliac crest markers in the static trial and during MRI collection enabled adjustment of the PSIS markers to match the upright standing position. This approach was feasible because of the low mean BMI of the participants ($< 17 \text{ kg/m}^2$), but it would have not been acceptable for children with larger BMI or adults, due to the effect of skin artefacts. Another limitation of the study is the

small population of CP children involved in the study. Although a larger clinical population would be necessary to generalize our findings, the heterogeneous diagnoses presented by the participants seem to suggest that our results are valid for all CP children that can walk without assistive device.

In conclusion, the present study has shown that HJC location errors propagate to all lower limb joint angles when using an IK approach, whereas using DK only hip and knee joint kinematics are affected. For the DK models, joint constraints increased the sensitivity of joint ROM to HJC location errors, whereas for the IK models changes in joint ROM and mean joint angles were similar between the 3-3-3-DoF-IK and 3-1-1-DoF-IK models. In both approaches (DK and IK) offsets in joint angles above 5° were observed which have the potential to mislead clinical interpretation [27,28]. In the absence of medical images to identify the HJC, predictive or functional methods with small errors in anterior-posterior and medial-lateral directions and scaling procedures minimizing HJC location errors in the anterior-posterior direction should be chosen to minimize the impact on joint kinematics.

Conflict of interest

Acknowledgements

Appendix A. Supplementary data

Supplementary data associated with this article can be found, in the online version, at http://dx.doi.org/10.1016/j.gaitpost.2017.06.002.

References

[1] F.M. Chang, J.T. Rhodes, K.M. Flynn, J.J. Carollo, The role of gait analysis in treating gait abnormalities in cerebral palsy, Orthop. Clin. North Am. 41 (2010) 489–506.

[2] M.P. Kadaba, H.K. Ramakrishnan, M.E. Wootten, Measurement of lower extremity kinematics during level walking, J. Orthop. Res. 8 (1990) 383–392.

[3] R.B. Davis, S. Õunpuu, D. Tyburski, J.R. Gage, A gait analysis data collection and reduction technique, Hum. Movement Sci. 10 (1991) 575–587.

[4] V.M. Zatsiorsky, Kinematics of Human Motion USA: Human Kinetics, (1998).

[5] E.S. Grood, W.J. Suntay, A joint coordinate system for the clinical description of three-dimensional motions: application to the knee, J. Biomech. Eng. 105 (1983) 136–144.

[6] M. Damsgaard, J. Rasmussen, S.T. Christensen, E. Surma, M. de Zee, Analysis of musculoskeletal systems in the AnyBody Modeling System, Sim. Model. Pract. Theory 14 (2006) 1100–1111.

[7] S.L. Delp, F.C. Anderson, A.S. Arnold, P. Loan, A. Habib, C.T. John, et al., OpenSim: open-source software to create and analyze dynamic simulations of movement, IEEE Trans. Biomed. Eng. 54 (2007) 1940–1950.

[8] T.W. Lu, J.J. O'Connor, Bone position estimation from skin marker co-ordinates using global optimisation with joint constraints, J. Biomech. 32 (1999) 129–134.

[9] S. Duprey, L. Cheze, R. Dumas, Influence of joint constraints on lower limb kinematics estimation from skin markers using global optimization, J. Biomech. 43 (2010) 2858–2862.

[10] S.L. Delp, A.S. Arnold, R.A. Speers, C.A. Moore, Hamstrings and psoas lengths during normal and crouch gait: implications for muscle-tendon surgery, J. Orthop. Res. 14 (1996) 144–151.

[11] L. Barber, C. Carty, L. Modenese, J. Walsh, R. Boyd, G. Lichtwark, Medial gastrocnemius and soleus muscle-tendon unit, fascicle, and tendon interaction during walking in children with cerebral palsy, Dev. Med. Child Neurol. (2017), http://dx.doi.org/10.1111/dmcn.13427 (in press) Paper is available online at http://onlinelibrary.wiley.com/doi/10.1111/dmcn.13427/ful l.

[12] L. Modenese, A.T. Phillips, Prediction of hip contact forces and muscle activations during walking at different speeds, Multibody Syst. Dyn. 28 (2012) 157–168.

[13] D.J. Saxby, L. Modenese, A.L. Bryant, P. Gerus, B. Killen, K. Fortin, et al., Tibiofemoral contact forces during walking, running and sidestepping, Gait Posture 49 (2016) 78–85.

[14] D.F. Graham, C.P. Carty, D.G. Lloyd, G.A. Lichtwark, R.S. Barrett, Muscle contributions to recovery from forward loss of balance by stepping, J. Biomech. 47 (2014) 667–674.

[15] V. Carbone, R. Fluit, P. Pellikaan, M. van der Krogt, D. Janssen, M. Damsgaard, et al., TLEM 2.0–A comprehensive musculoskeletal geometry dataset for subject-specific modeling of lower extremity, J. Biomech. 48 (2015) 734–741.

[16] L. Modenese, A.T. Phillips, A.M. Bull, An open source lower limb model: hip joint validation, J. Biomech. 44 (2011) 2185–2193.

[17] S.L. Delp, J.P. Loan, M.G. Hoy, F.E. Zajac, E.L. Topp, J.M. Rosen, An interactive graphics-based model of the lower extremity to study orthopaedic surgical procedures, IEEE Trans. Biomed. Eng. 37 (1990) 757–767.

[18] A. Cappozzo, F. Catani, U.D. Croce, A. Leardini, Position and orientation in space of bones during movement: anatomical frame definition and determination, Clin. Biomech. (Bristol, Avon) 10 (1995) 171–178.

[19] A. Cereatti, V. Camomilla, G. Vannozzi, A. Cappozzo, Propagation of the hip joint centre location error to the estimate of femur vs pelvis orientation using a constrained or an unconstrained approach, J. Biomech. 40 (2007) 1228–1234.

[20] H. Kainz, C.P. Carty, L. Modenese, R.N. Boyd, D.G. Lloyd, Estimation of the hip joint centre in human motion analysis: a systematic review, Clin. Biomech. (Bristol, Avon) 30 (2015) 319–329.

[21] R. Stagni, A. Leardini, A. Cappozzo, M. Grazia Benedetti, A. Cappello, Effects of hip joint centre mislocation on gait analysis results, J. Biomech. 33 (2000) 1479–1487.

[22] H. Kainz, L. Modenese, D.G. Lloyd, S. Maine, J. Walsh, C.P. Carty, Joint kinematic calculation based on clinical direct kinematic versus inverse kinematic gait models, J. Biomech. 49 (2016) 1658–1669.

[23] G. Valente, L. Pitto, D. Testi, A. Seth, S.L. Delp, R. Stagni, et al., Are subject-specific musculoskeletal models robust to the uncertainties in parameter identification? PLoS One 9 (2014) e112625.

[24] G. Wu, S. Siegler, P. Allard, C. Kirtley, A. Leardini, D. Rosenbaum, et al., ISB recommendation on definitions of joint coordinate system of various joints for the reporting of human joint motion—part I: ankle, hip, and spine, J. Biomech. 35 (2002) 543–548.

[25] A. Leardini, Z. Sawacha, G. Paolini, S. Ingrosso, R. Nativo, M.G. Benedetti, A new anatomically based protocol for gait analysis in children, Gait Posture 26 (2007) 560–571.

[26] A. Leardini, A. Cappozzo, F. Catani, S. Toksvig-Larsen, A. Petitto, V. Sforza, et al., Validation of a functional method for the estimation of hip joint centre location, J. Biomech. 32 (1999) 99–103.

[27] J.L. McGinley, R. Baker, R. Wolfe, M.E. Morris, The reliability of three-dimensional kinematic gait measurements: a systematic review, Gait Posture 29 (2009) 360–369.

[28] R. Baker, J.L. McGinley, M. Schwartz, P. Thomason, J. Rodda, H.K. Graham, The minimal clinically important difference for the Gait Profile Score, Gait Posture 35 (2012) 612–615.